International Journal Of Biology and Biological Sciences Vol. 4(1), pp. 001-018, April 2015
Available online at http://academeresearchjournals.org/journal/ijbbs
ISSN 2327-3062 ©2015 Academe Research Journals

Full Length Research Paper

Genotoxicity and ultrastructural studies of the effect of cisplatin on the cortex of kidney of albino male mice

Azza A. Attia[1]*, Cecil A. Matta[1] and Hanan A. Khaliffa[2]

[1]Zoology Department, Faculty of Science, Alexandria University, Egypt.
[2]Faculty of Science, Omar Elmokhtar University, Lybia.

Accepted 11 September, 2014

Cisplatin is still a frequently used chemotherapeutic agent, despite its frequent adverse effects, including nephrotoxicity. The present work was done to investigate its harmful effects on the tissue kidney of the male mice. Two groups of mice were injected intraperitoneally with 0.5 ml cisplatin at doses of 0.15 and 0.3 mg/kg BW, two times/week, for four consecutive weeks. The third group animals was injected with 0.5 ml saline solution as a vehicle, and considered as a control. Chromosomal aberrations test, DNA assay and ultrastructural studies in the tissue of kidney were evaluated. The results revealed that depending on the dose response, there was an increase in the mortality rate and decrease in the body weights of experimental mice treated with the two dose levels of cisplatin. The chromosomal aberrations include deletion, centric fusion and stickiness, indicating the positive clastogenic effect of cisplatin. Severe DNA damage was more prominent in the tissue kidney of mice administered with 0.3 mg/kg BW cisplatin. Histologically, cisplatin caused severe structural alterations including destruction in the renal tubular cells, and presence of focal hemorrhage in between the tubules. The glomeruli exhibited shrinkage of the glomerular tuft and dilatation in the urinary spaces. At the ultrastructural level, severe atrophy in the glomeruli, rupture of Bowman's capsule and dilatation in the urinary space were observed. At the proximal conpluted tubules, the basal infoldings appeared short and flattened, and large vacuoles were noticed in the cytoplasm. Mostly, the nuclei were pyknotic, the mitochondria were pleomorphic, and there was an increase in the primary and secondary lysosomes. In the distal convoluted tubule cells, the nuclei were mostly pyknotic.

Key words: Cisplatin, glomeruli, genotoxicity, renal tubules, chromosomal aberrations, nephrotoxicity.

INTRODUCTION

It is well known that use of chemotherapy in the treatment of cancer has opened new possibilities for improvement of the quality of life of cancer patients (Chandrasekar et al., 2006). Chemotherapy involves the use of chemical agents to stop the growth and eliminate cancer cells even at distant sites from the origin of primary tumor. The chemotherapeutic agents can be divided into several categories: Alkylating agents (for example, cyclophosphamide), antibiotics which affect nucleic acids (for example, bleomycin), platinum compounds (for example, cisplatin), mitotic inhibitors (for example, vincristine), antimetabolites (for example, 5-flurouracil), biological response (for example, interferon), and hormone therapies (for example, tamoxifen) (Holland et al., 1997).

Cisplatin (cis-diamminedichloroplatinum) as an efficient platinum-derived alkylating agent is one of the most important chemotherapeutic agents ever introduced. It is used for a wide spectrum in human malignancies (Shah and Dizon, 2009; Zhang et al., 2010). However, its major side effects, nephrotoxicity and hepatotoxicity are the main limiting factors of its clinical use for long term treatment (Mansour et al., 2006). Miller et al. (2010) found that the adverse effects of cisplatin could cause

*Corresponding author. E-mail: azzzaatia@hotmail.com.

nephrotoxicity.

Kidneys are dynamic organs and represent the major control system maintaining the body haemostasis; they are affected by many chemicals and drugs (Ajith et al., 2007). Ali and Al-Moundhri (2006) found that cisplatin could accumulate in the renal tubular cells approximately five times its extracellular concentration. Saad et al. (2009) indicated that cisplatin induced damage in kidney genomic DNA, lipid peroxidation, inhibition of antioxidant enzymes and alterations of biochemical parameters in plasma and kidney of rats.

After application of cisplatin, damage to DNA may result in DNA fragmentation, chromosomal breaks, and micronucleus formation causing genomic instability, and may lead to mutagenesis, carcinogenesis, or finally to apoptotic cell death (Nersesyan et al., 2003; Yoshida et al., 2006). Florea and Büsselberg (2011) explained that cisplatin could induce cytotoxicity by interference with transcription and/or DNA replication mechanisms.

Sahu et al. (2011) indicated that the toxic effects of CP occur through increased oxidative stress and apoptosis. Domitrovic et al. (2014) found that cisplatin administration resulted in a severe nephropathy, accompanied by impaired histological features of the kidneys. Park et al. (2002) explained that cisplatin could induce apoptosis via activation of mitochondrial signaling pathways. Custódio et al. (2009) added that cisplatin causes an increase in the sensitivity of mitochondria to Ca^{2+}-induced mitochondrial permeability transition, interference with mitochondrial bioenergetics by increasing mitochondrial inner membrane permeabilization to H^+ but does not significantly affect H_2O_2 generation by mitochondria. Therefore, the aim of this study was to evaluate the chromosomal aberration in the bone marrow cells, and the extent of DNA damaging in the tissue kidney. Histopathological and ultrastructural changes of the effect of cisplatin on the cortical regions of the kidney of mice were also investigated.

MATERIALS AND METHODS

Animal study

Forty five healthy adult male albino mice were obtained from the Faculty of Agriculture, Alexandria University, Alexandria, Egypt. They were of 3 months old, and weighing 28-32 g each, when the experimentation commenced. All animals were housed in the usual stainless steel cages (5 mice/cage), which were cleaned day by day continuously. They adapted to the controlled environmental conditions at room temperature of 25 ± 2°C, and normal photoperiod of 12 h/day. Also, they were allowed free access to food (wheat, bread) and drinking water *ad libitum*.

Drug preparation

Cisplatin was purchased from the pharmacy under the international trade name cisplatin MERCK®. It was manufactured by Oncoten Pharma Production GmbH, Rodleben-Germany. Two different dose levels were prepared according to the equivalent prescribed dose for human (5 and 10 mg/Kg body weight) (Mansour et al., 2006; Abdelwahab et al., 2011), which were calculated to be 0.15 and 0.3 mg/kg BW/mice respectively.

Treatment

All mice were divided into two experimental groups and one control (each of 14), according to their approximately equal body weights. Two experimental group mice were injected intraperitoneally, two times/week, for 4 consequtive weeks with 0.5 ml of cisplatin at a dose level of 0.15 and 0.3 mg/kg BW. The third group mice was considered as a control and administered with 0.5 ml saline solution (0.9% NaCl), two times/week, for four consecutive weeks.

Macroscopic examination

During the experiment, all treated mice and the control were carefully examined in order to depict any apparent external changes and/or sign of toxicity. The number of dead mice occurring among them was counted and the percentage of mortality was calculated.

Body weight and weight change

At the end of the experiment, the body weight change (%) was estimated by dividing the final body weight / initial body weight × 100.

The chromosomal aberration test

Five mice of each control and the treated mice were used for studying the chromosomal aberrations. According to the method of Preston et al. (1987), 24 h after administration of the last dose of cisplatin, mice were injected intravenously with 0.5 mg/kg colchicines, 2 h prior to sacrifice. Femurs of each mouse were dissected out quickly, and bone marrow cells were collected by flushing in KCl (0.075 M) and incubated at 37°C for 25 min. The collected bone marrow cells were centrifuged at 2000 rpm for 10 min, and fixed in acetic acid:methanol (1:3 respectively). Centrifugation and fixation were repeated four times at an interval of 15 min each. The cells were resuspended in a small volume of fixative, dropped onto slides, flame-dried and stained with 5% Giemsa stain for 3-5 min, washed in distilled water to remove excess stain. The best spread metaphase cells were selected, and the structural chromosomal aberrations were scored in 100 metaphases for each animal to a total number of 150 metaphases to obtain the total number of chromosomal aberration.

Histopathological study

At the end of the experiment, mice of the experimental

Table 1. % of mortality and body weight change of mice treated with the two doses of cisplatin for four weeks.

Experimental groups	No. of mice	No. of dead mice	% of mortality	Mean of body weight (g)		% of Body weight change
				Initial	Final	
Control mice	40	0	0.0	29.80 ± 0.76	30.85 ± 0.17[a]	3.52 ± 1.64[a]
5 mg/kg bw cisplatin	40	6	15.0	28.28 ± 0.24	26.64 ± 0.29[b]	-5.8 ± 1.29[b]
10 mg/kg bw cisplatin	40	13	32.5	30.33 ± 0.22	25.07 ± 0.28[c]	-17.34 ± 0.97[c]

Data are expressed as mean ± SE. a, b, c: means that there is no significant difference at values of P ≤ 0.05, among the tested groups when compared to the control.

groups and the control were dissected out quickly. Small slices of the cortical region of kidney were taken immediately and fixed overnight in a freshly prepared 10% formalin solution. The fixed specimens were processed by the usual recognized histological methods of dehydration, clearing by xylene and embedding in paraffin wax (Bancroft and Gamble, 2002). Serial sections were cut at 5-6 µm thickness, stained by hematoxylin-eosin (H&E), examined and photographed by the light microscopy.

Ultrastructural investigation

Very small slices of the cortex of kidney of both control and cisplatin–treated mice were immediately fixed in 2% $_4F_1G$, then rinsed in 0.1 M phosphate buffer (pH = 7.4) at 4°C for around 1 h, then rinsed in 0.1 M phosphate buffer (pH 7.4). This was followed by post-fixation using 1% buffered OsO4 (osmium tetroxide) for 1-2 h at 4°C, then the specimens were washed with phosphate buffer for several times for 30 min, after which they were dehydrated in ascending grades of ethanol concentration. Tissues were then treated with propylene oxide and embedded in a mixture of 1: 1 of Epon-Araldite. Specimens were embedded in pre-dried gelatine capsule (dried in the oven at 37°C for 1 h before use). Polymerization was done in the oven at 65°C for 24 h. Ultrathin sections obtained from such specimens were with a glass knife on LKB ultramicrotome, mounted on 200 mesh naked copper grids, doubled stained with uranyl acetate and lead citrate (Hayat, 2000). Sections were examined by using Jeol 100CX transmission electron microscope at the Faculty of Science, Alexandria University, Alexandria, Egypt.

DNA analysis

According to the method of Saad et al. (2009), the electrophoretic DNA was assayed for the tissue kidney (five mice of each experimental group and the control).

Statistical analysis

Statistical analysis for all data was done using the SPSS software package version 17.0, and the results were expressed as the mean ± Standard Error (SE). Then, they were analyzed statistically using one-way analysis of variance (ANOVA). All tests were carried out at a significant level of $P<0.05$ (P= probability value). Further, analyses of the data were performed with the least significant difference (LSD) to determine which sample was significantly different from the control.

RESULTS

External signs of toxicity

The results revealed that the signs of toxicity were more prominent in mice treated with 0.3 mg/kg bw cisplatin, where fall of body hair and decrease in the body weight were prominent. The mortality rate in mice treated with 0.15 mg/kg BW cisplatin was 15%, increasing to 32.5% in those treated with 0.3 mg/kg BW. Depending on dose response, the body weights of cisplatin-treated mice were significantly decreased ($p\leq0.05$) versus the control mice (Table 1).

The chromosomal aberrations

The appearance of chromosomes was studied in the bone marrow metaphase of mitotic division. The chromosome complement of the mouse is composed of 2n = 40 chromosomes, including 19 pairs of autosomes and a pair of sex chromosome (XX, XY for female and male respectively). All chromosomes are acrocentric (Figure 1a). Depending on dose response, the results indicated that cisplatin induced various chromosomal aberrations in the bone marrow cells of mice. These aberrations comprised 4 types namely, gaps (0.4%) (Figure 2a), deletion (0.4%) (Figure 2b), fragmentation (0.6%) (Figure 2c), and centromeric attenuation (0.2%) (Figures 2d and 3b). End to end association in the chromosome is induced by general stickiness of chromosomes (Figure 2d). In addition, there was centic fusion (Figure 3a), ring formation (Figures 2b and 3a), chromosomal stickiness (Figure 3c) and pulverized chromosome (Figure 3d).

DNA assay

The genomic DNA extracted from kidney tissues of the different experimental groups showed that treatment with

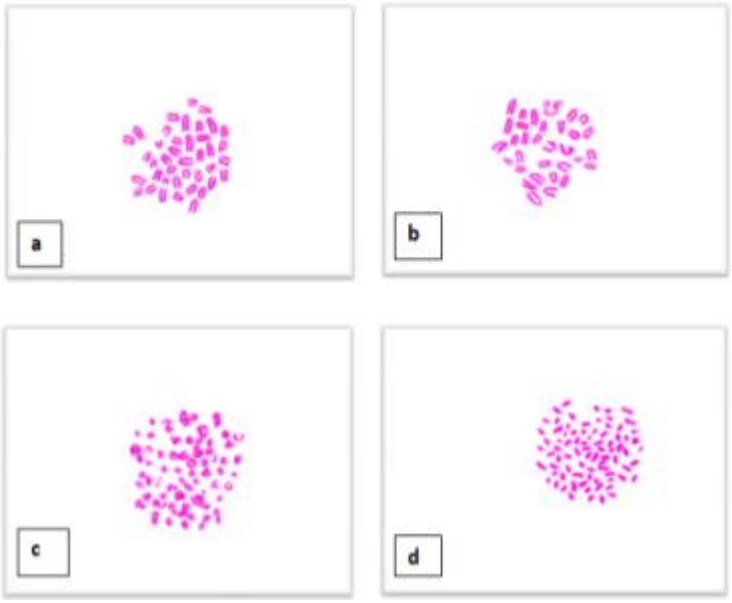

Figure 1. Light micrographs of metaphase of mouse bone marrow cells showing: a) normal acrocentric chromosomes; b) hypodiploidy; c) polyploidy; d) endomitosis.

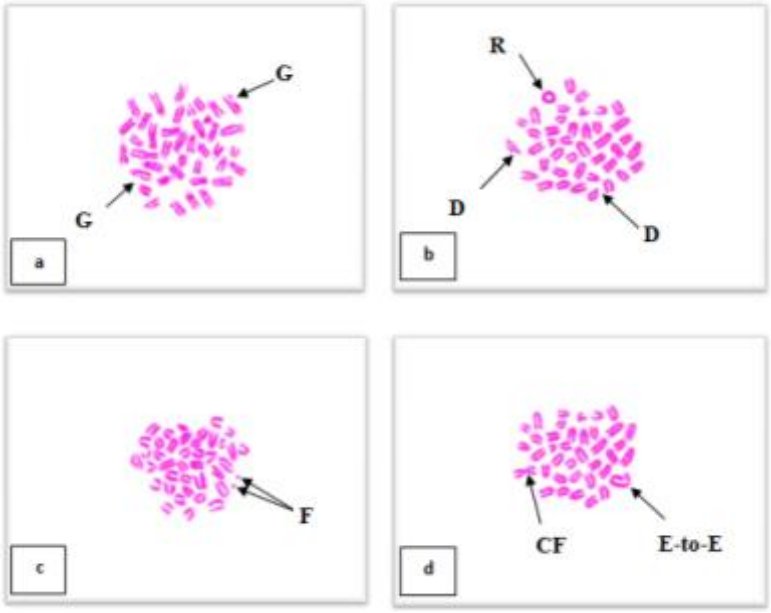

Figure 2. Light micrographs of metaphase chromosomal aberrations of mouse bone marrow cells showing: a) gaps (G); b) ring (R), deletion (D); c) fragmentation (F); d) centric fusion (CF) and end-to-end association (E-to-E).

low-dose cisplatin (0.15 mg/kg BW) caused a partial degradation of genomic DNA characterized only by smearing of DNA fragments (Figure 4, Lanes B, C), compared with the DNA isolated from control samples (Figure 4, Lane A) which showed DNA intact. Whereas, the DNA of high-dose treated mice was evident that administration of cisplatin exhibited dramatic complete degradation of genomic DNA (Figure 4, Lanes D, E).

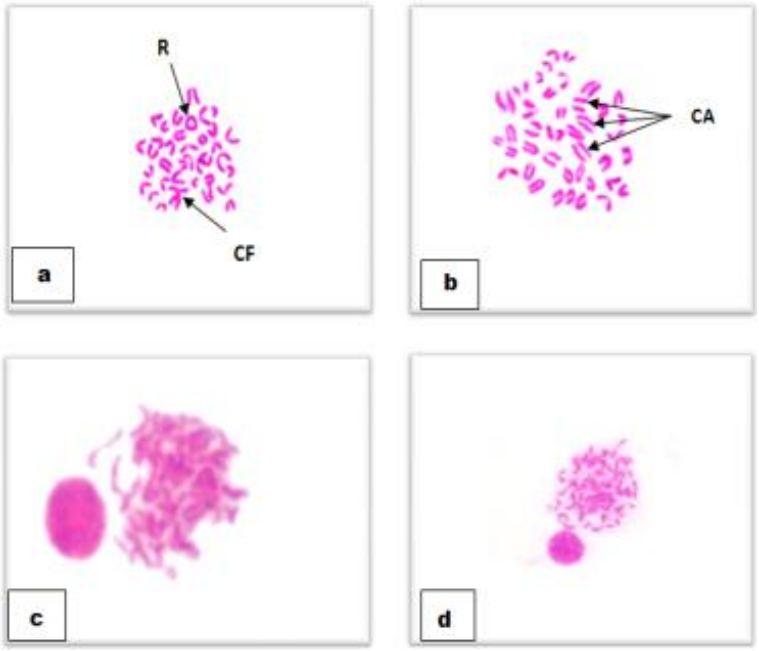

Figure 3. Light micrographs of metaphase chromosomal aberrations of mouse bone marrow cells showing: a) ring (R); centric fusion (CF); b) centric attenuation (CA); c) stickiness; d) pulverized cells.

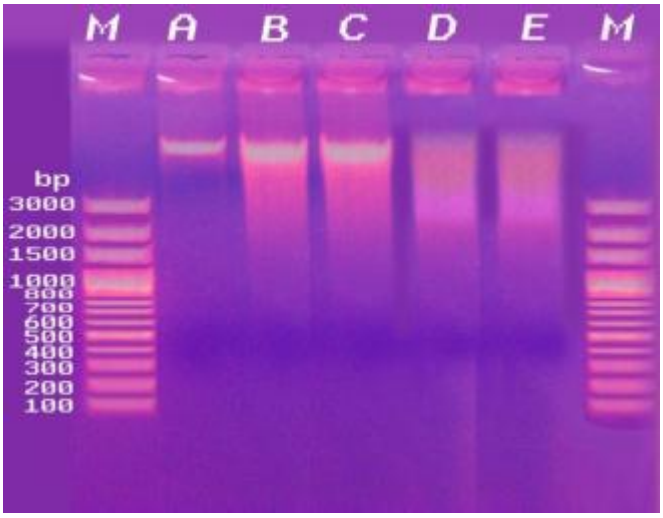

Figure 4. Gel electrophoresis photograph showing the genomic DNA of kidney of control and treated mice. Lane M: DNA marker; Lane A: Control; Lane B, C: 0.15 mg/kg BW cisplatin; Lane D, E: 0.3 mg/kg BW cisplatin.

Histoplathological findings

Section in the kidney of control mice is found to divide into an outer dark cortex and an inner light medulla. The renal cortex is composed mainly of millions of functional units (nephrons), each one consisting of two major components - the renal corpuscles and the renal tubules. The renal corpuscle consists of a tuft of capillaries, the glomerulus, which is surrounded by a double-walled epithelial capsule called the Bowman's capsule, and the urinary space (Figure 5).

The proximal convoluted tubules (PCT) possess narrow

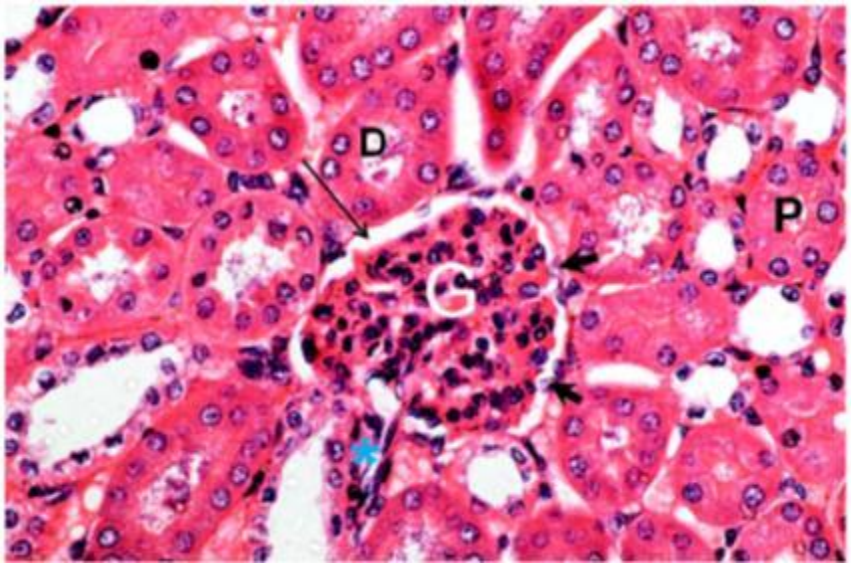

Figure 5. Light micrograph in the renal cortex of control mouse revealing the glomerulus (G) with distinct urinary space (arrow); notice: the flattened nuclei (arrow head) lining the Bowman's capsule; proximal convoluted tubule (P); distal convoluted tubule (D), × 400.

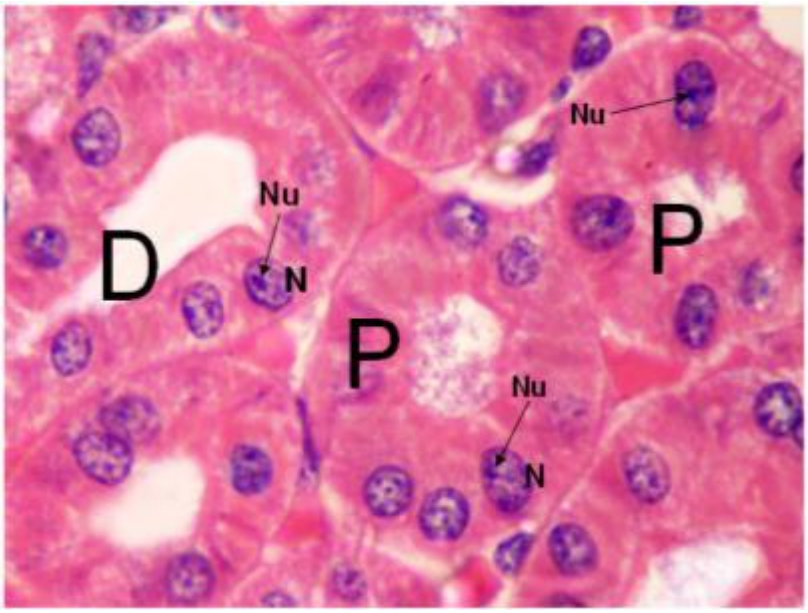

Figure 6. Light micrograph of the renal tubules in kidney of control mouse revealing proximal convoluted tubules (P) lined by high cuboidal or pyramidal cells, having spherical basally located nuclei (N) and prominent nucleoli (Nu); distal convoluted tubule (D) are lined by cuboidal cells, having rounded-shaped nuclei (N), × 1000.

lumen and their cells have large spherical nuclei, and centrally located prominent nucleoli. The apical surfaces of these cells that face the lumen exhibit abundant microvilli which form the so called brush border. The distal convoluted tubules (DCT) have wide lumina and are bordered by cubical or low columnar epithelial cells, having flattened small nuclei (Figure 6).

Ultrastructurally, in the glomerulus, the parietal layer of

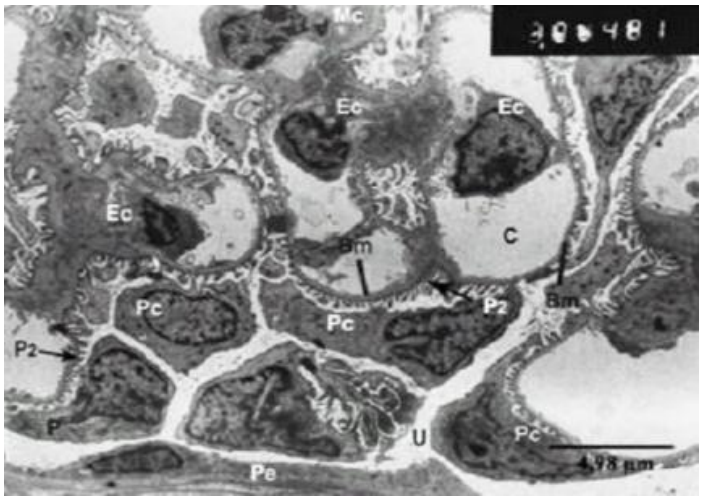

Figure 7. Electron micrograph of the renal corpuscle in the kidney of control mouse showing: the blood capillaries (C); endothelial cells (Ec); basement membrane (Bm); podocytes (Pc); secondary foot process (P2); the urinary space (U); the mesangial cells (Ms); the parietal (Pe), × 2000.

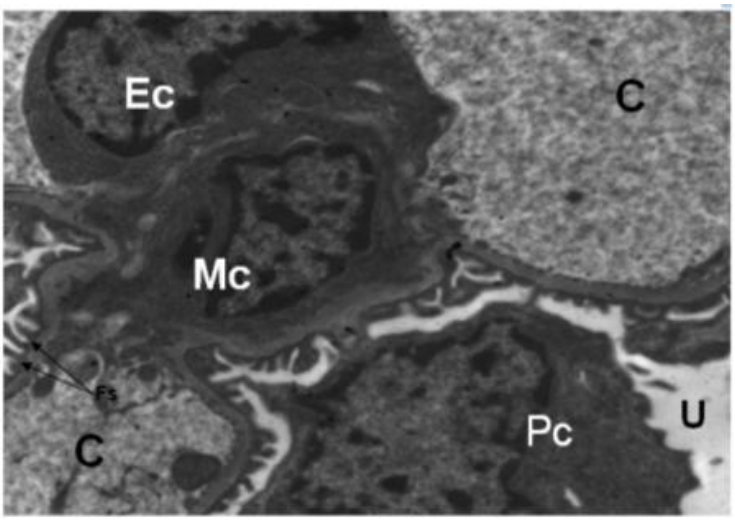

Figure 8. Electron micrograph of the renal corpuscle in the kidney of control mouse showing the mesengial cell (Mc) interposed between the blood capillaries (C); podycytes (Pc) are suspended in the urinary space (U), heterochromatic large nucleus (N), filtration slits (fs), × 4000.

Bowman's capsule consists of a layer of simple sequamous cells which bulges into the urinary space in the region of their nuclei (Figure 7). The visceral layer of the Bowman's capsule is formed of modified cells called the podocytes which are suspended in the urinary space. These cells are basically stellate with several radiating primary foot processes and secondary processes called the pedicles. These secondary foot processes are in direct contact with the renal filtration barrier, and the ending of these processes interdigitate to cover the glomerular basement membrane and are separated by gaps of uniform with the "filtration slits" (Figures 7 and 8). The pores, between the pedicles are opened into the urinary space.

The ultrastructural examination of the proximal tubule cells in the cortex of the kidney of control mice showed that they have highly polarized domains in the plasma membrane. The apical domain contains long microvilli

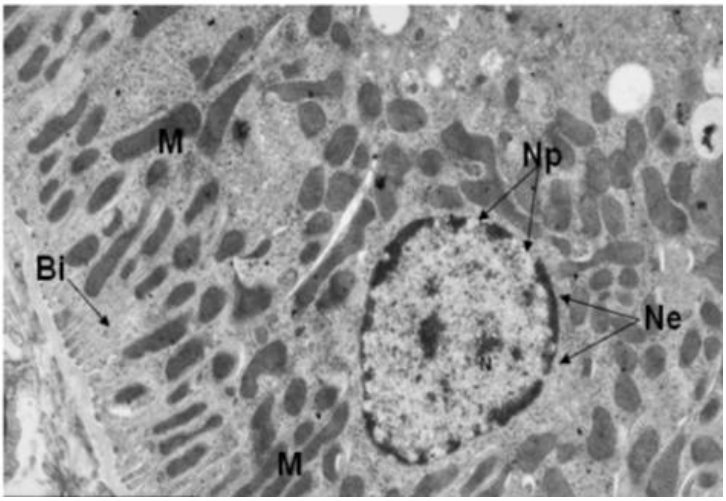

Figure 9. Electron micrograph in a proximal convoluted tubule cell in the kidney of control mouse showing the nucleus (N) and the nuclear envelope (Ne); nuclear pores (Np); mitochondria (M); Note: the basal infolding (Bi), × 7500.

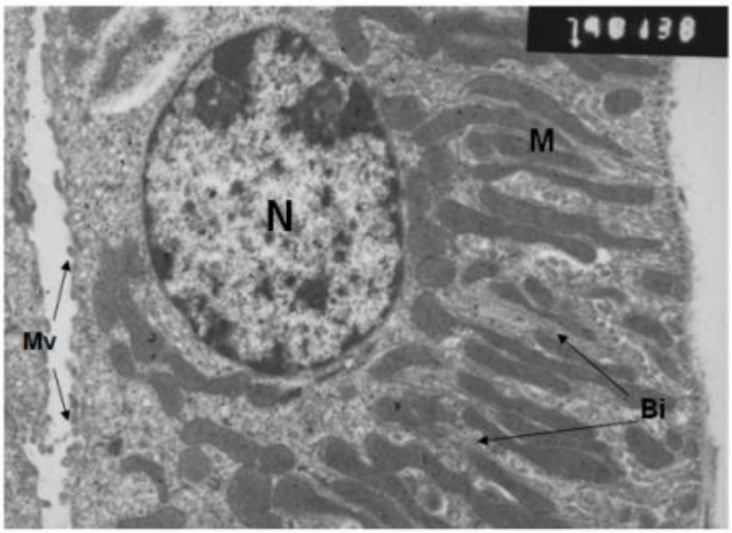

Figure 10. Electron micrograph in a distal convoluted tubule cell in the kidney of control mouse showing, apical spherical nuclei (N); Note: the mitochondria (M); short microvilli (Mv) and the basal infoldings (Bi), × 7500.

forming a conspicuous brush border that lines the laming surface, while the basal plasma membrane domain, adjacent to the basement membrane is complex and contains numerous cytoplasmic folds project into the basal extracellular space. The nuclei of these cells are roughly spherical in shape. The apical and mid regions of these cells contains rounded-shaped mitochondria, and the basal part contains dense and elongated mitochondria which are lodged in between the basolateral infoldings (Figure 9).

The distal convoluted tubule cells are of low columnar shaped-structure, and the luminal plasma membrane forms occasional short and blunt microvilli. These cells have rounded-shaped nuclei which are commonly located toward the apical surface of the tubular cells. The mitochondria at the apical mid regions of the tubular cells are mostly rounded in shape and small in size; while many filamentous and elongated mitochondria are located at the basal part (Figure 10).

Sections in the cortical region of kidney of mice treated

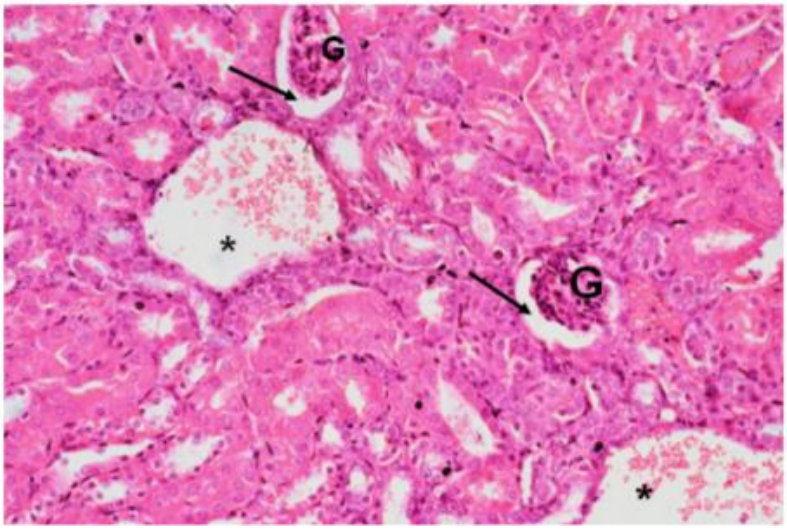

Figure 11. Light micrograph of the renal cortex in the kidney of mouse treated with 0.15 mg/kg BW cisplatin showing, atrophy of glomeruli (G); dilated urinary spaces (arrows); congested blood vessels (*), × 200.

Figure 12. Light micrograph of the renal cortex in kidney of mouse treated with 0.15 mg/kg BW cisplatin showing, abnormal morphological appearance; Note: the glomerulus displays shrunken (G); dilatation in the urinary space (Us); marked tubular necrosis (*); arrows point at detached cellular debris, × 400.

with 0.15 mg/kg BW cisplatin showed the appearance of many dilated and congested blood vessels, and the malpighian corpuscles were atrophied and shrunken (Figure 11). Both the proximal and the distal convoluted tubules displayed numerous abnormalities including damages in their morphology and cellular arrangement including loss of the tubular epithelial cells, dilatation of lumen and necrotic epithelial cells (Figure 12).

Ultrastructurally, in the renal corpuscles, mild partial collapse and the red blood cells were observed in the capillary lumen. The podocyte cells were shrunken and their cytoplasmic extensions were fragmented. The secondary foot processes or pedicels of podocytes were disordered with focal fusion (Figure 13), and sometimes

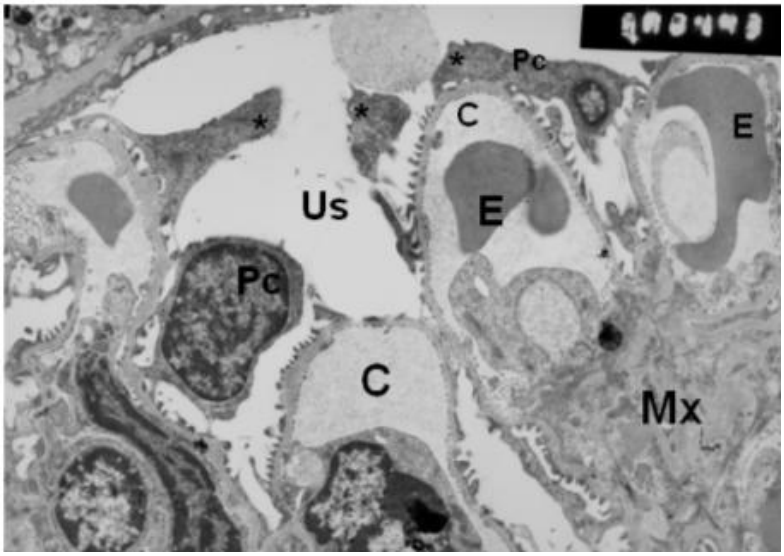

Figure 13. Electron micrograph of the renal corpuscle in the kidney of mouse treated with 0.15 mg/kg BW cisplatin showing, narrow of capillaries (C); erythrocytes (E); podocytes (Pc) exhibite shrunken and their cytoplasmic extensions are fragmented (*); mesangial matrix (Mx), × 5000.

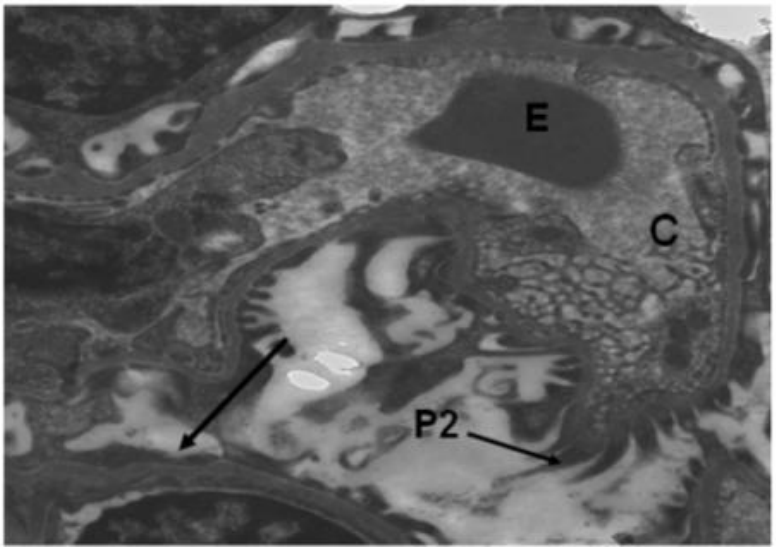

Figure 14. Electron micrograph of the renal corpuscle in the kidney of mouse treated with 0.15 mg/kg BW cisplatin showing, secondary foot processes (P2); formation a sheet of podocyte cytoplasm (arrows); wide capillary (C) contains erythrocyte (E), X 5000.

appear as marked balloning structure. The secondary foot processes of podocytes were longer at certain places. The basement membrane of these cells was thickened and was not uniform in its appearance (Figure 14). The proximal convoluted tubule showed little ultrastructural alterations in both the nuclei and cytoplasm of these cells. The basement membrane became slightly thickened at certain intervals with disorganized basal infoldings. The lateral intercellular space was relatively wide. The cytoplasm contains large vacuoles, and the mitochondria attained pleomorphic shape, and exhibited irregular distribution (Figure 15). In the distal tubule cells, few short apical microvilli were projected toward the lumen, and their nuclei were irregularly outlined. The

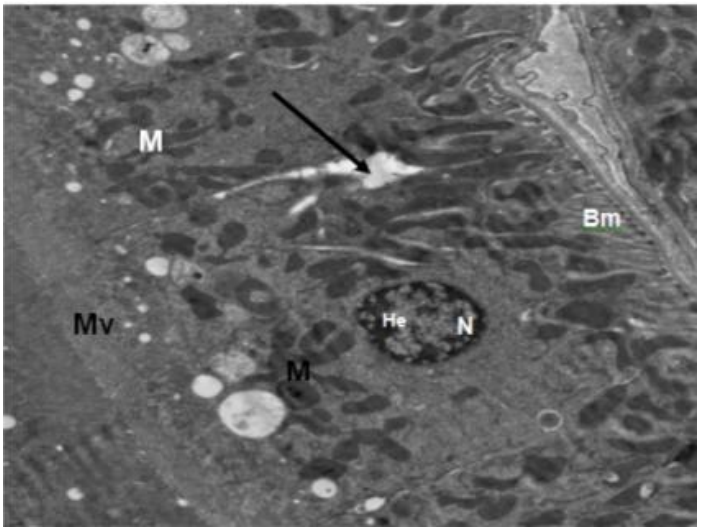

Figure 15. Electron micrograph in the proximal convoluted tubules in kidney of mouse treated with 0.15 mg/kg BW cisplatin showing, short microvillus border (Mv); pyknotic nucleus (N); Note: the pleomorphic mitochondria (M); arrow points at the intercellular space, × 2500.

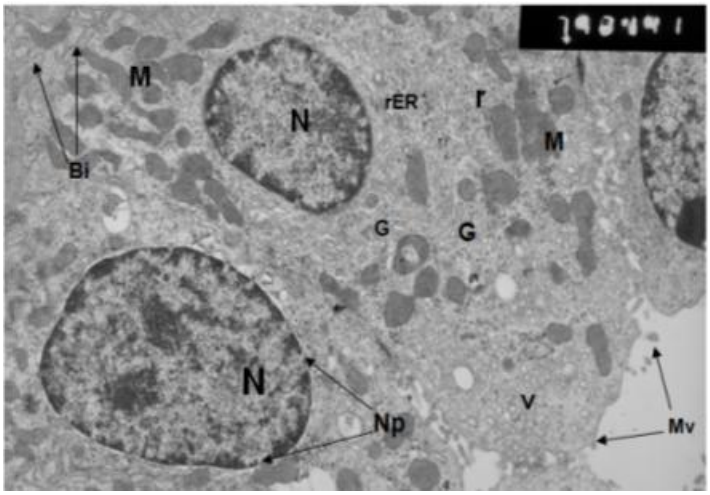

Figure 16. Electron micrograph of the distal convoluted tubule cell in the kidney of mouse treated with 0.15 mg/kg BW cisplatin showing, rupture microvilli (arrows); pleomorphic mitochondria (M); nuclei (N) with slightly irregular nuclear outline; basal infolding (Bi); Golgi apparatus (G); low rough endoplasmic reticulum (rER); pleomorphic mitochondria (M); pinocytotic vesicles (v), × 7500.

cytoplasm contains few small vacuoles, and the mitochondria were aggregated at the basal cytoplasmic part (Figures 16 and 17). Sections in the cortical region of kidney of mice treated with 0.3 mg/kg BW cisplatin showed marked congestion in the blood vessels, and the renal tubules had lost their regular shape, sloughing of cells and complete lysis of their cytoplasm were observed (Figure 18). Focal inflammatory cells infiltrated were observed around the glomeruli, and most of the glomeruli exhibited shrinkage of the glomerular tuft and dilatation in the urinary spaces (Figure 19). Further, the results revealed marked degeneration in both the proximal and distal convoluted tubules, and the presence of observable necrotic areas (Figure 20).

At the ultrastructural level, the lumen of the glomerular capillaries was highly dilated and it showed the presence

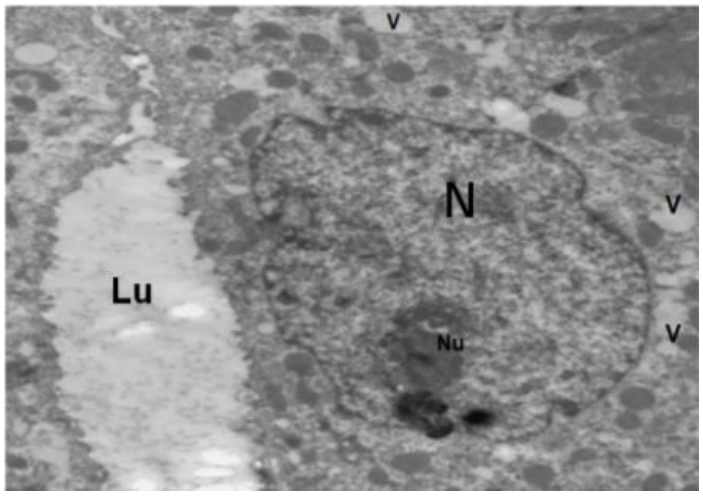

Figure 17. Electron micrograph of the distal convoluted tubule in the kidney of mouse treated with 0.15 mg/kg BW cisplatin showing, the irregular-shaped nucleus (N); Note: the presence of vacuoles (V) in the cytoplasm, × 2000.

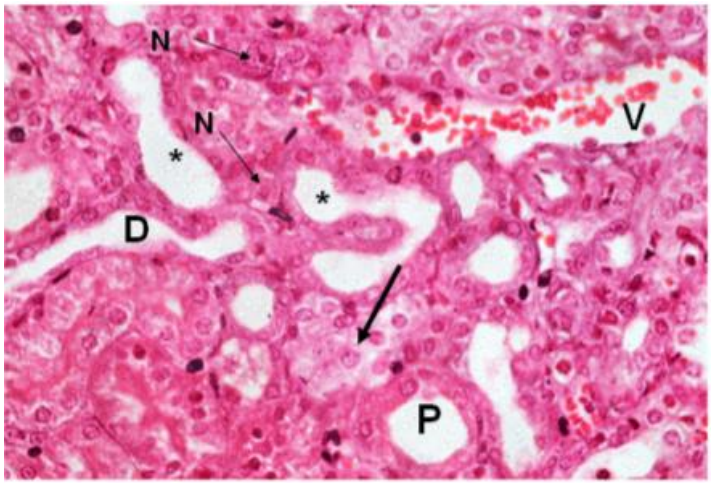

Figure 18. Light micrograph of the renal cortex in the kidney of mouse treated with 0.3 mg/kg BW cisplatin, showing the prominent distortion in the proximal (P) and the distal (D) convoluted tubules; dilatation in the lumen (*) of the tubules, loss of the epithelial lining (arrow), congested blood vessels (V), × 400.

of erythrocytes (Figure 21). The secondary foot processes were hypertrophied and uptake ballooned-like structure (Figure 22). The nuclei of most PCT cells were pyknotic (Figures 23 and 24). The mitochondria displayed characteristic feature of injury such as swelling, disappearance of cristae, and they were not arranged in the usual manner as in the control (Figure 25). In addition, large vacuoles were observed in the apical part of their cytoplasm, and there was prominent increase in the primary and secondary lysosomes (Figures 23 and 25). In the distal convoluted tubule cells, the nuclei were mostly pyknotic, and the nucleoli were absent in most of them. In the cytoplasm of these cells, the mitochondria had lost their typical arrangement, where there were no focal elongated mitochondria in the basal infoldings (Figure 26).

DISCUSSION

Cisplatin is a widely used and effective anticancer drug, associated with significant dose-limiting toxicities including nephrotoxicity and neurotoxicity. Depending on

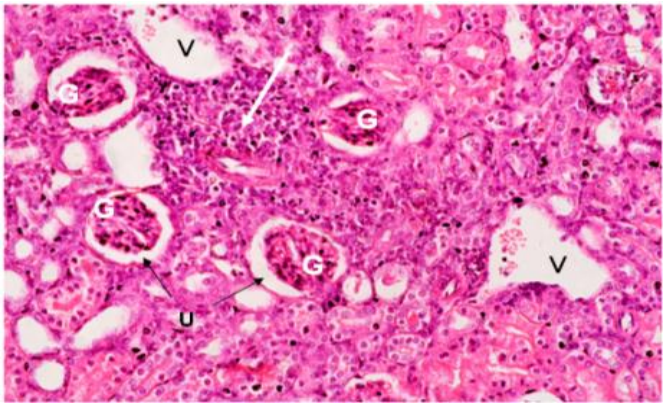

Figure 19. Light micrograph of the renal cortex in kidney of mouse treated with 0.3 mg/kg BW cisplatin, showing shrunk glomeruli (G) with densely basophilic nuclei. Also, note: dilatation of urinary space (U); focal inflammatory cells infiltration (white arrow); dilated vein (V), × 200.

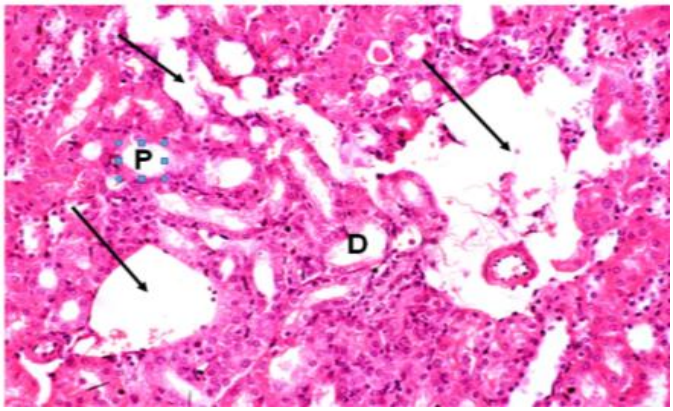

Figure 20. Light micrograph of the renal cortex in the kidney of mouse treated with 0.3 mg/kg BW cisplatin, showing disruption in the appearance of proximal (P) and distal (D) convoluted tubules; arrows point at intercellular space between the tubules, × 200.

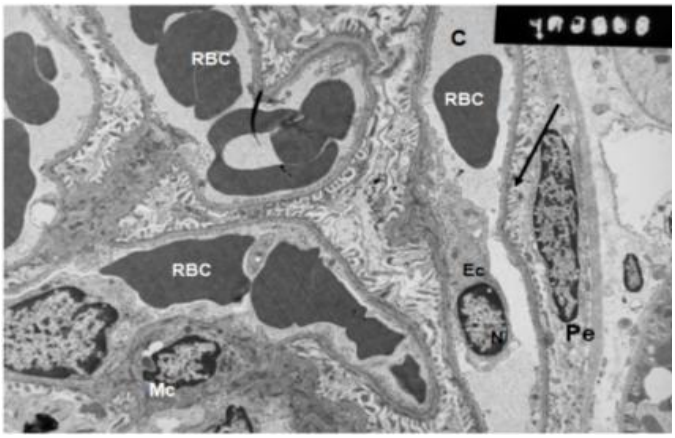

Figure 21. Electron micrograph of the renal corpuscle in the kidney of mouse treated with 0.3 mg/kg BW cisplatin, showing adhesion between parietal layer (Pe) and the visceral layer (arrow); Mesangial cell (Mc); Note: the wide congested capillaries (C), erythrocytes (RBC), X 5000.

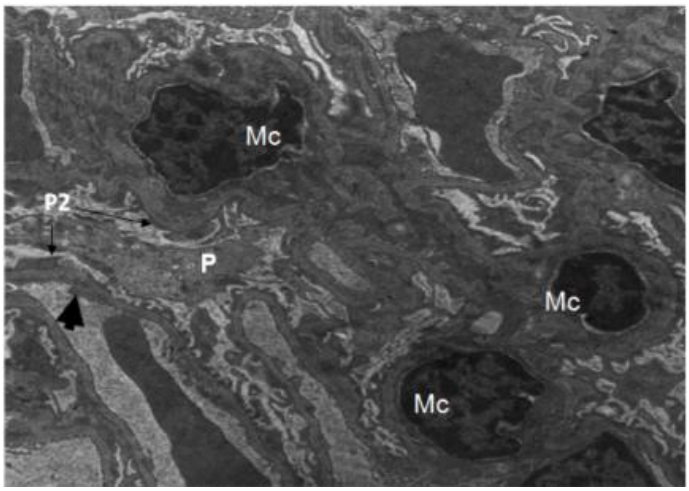

Figure 22. Electron micrograph of the renal corpuscle in the kidney of mouse treated with 0.3 mg/kg BW cisplatin, showing disorganized foot processes (P) in the podocyte; Note: the lack in the endothelial fenestrate (arrow head); the Mesangial cells (Mc), × 2500.

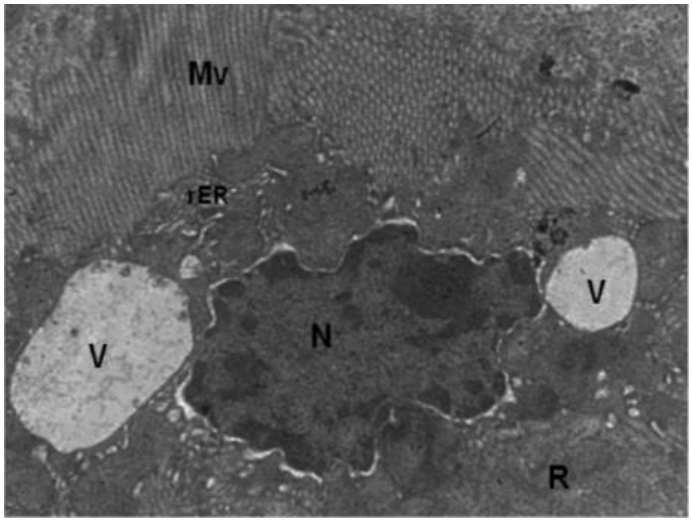

Figure 23. Electron micrograph of a proximal convoluted tubule cell in the kidney of mouse treated with 0.3 mg/kg BW cisplatin, showing a pyknotic nucleus (N), having highly folded nuclear envelop (NP); Note: the presence of large vacuoles (V) in the cytoplasm; microvilli (Mv), × 3000.

the dose response of cisplatin, the results revealed an increase in the mortality rate, while there is marked significant decrease in the body weight. Similarly, Dzagnidze et al. (2007) noticed that mice injected with a single i.p dose of cisplatin (2 and 10 mg/kg BW) caused marked increase in the rate of mortality. Several investigators (Saad et al., 2009; Domitrovic et al., 2014; Abdelmeguid et al., 2010) reported that cisplatin had been shown to decrease the total body weight of mice and rats. This decrease in the body weight might be due to the decrease in appetite and the enhancement of the catabolic rate which is considered as the obvious side effects of the chemotherapy (Hassan et al., 2010). Atessahin et al. (2005) explained that body weight loss might be due to the drug toxicity or the gastrointestinal toxicity and thereby reducing ingestion of food (Tikoo et al., 2007).

The bone marrow cells with structural chromosomal

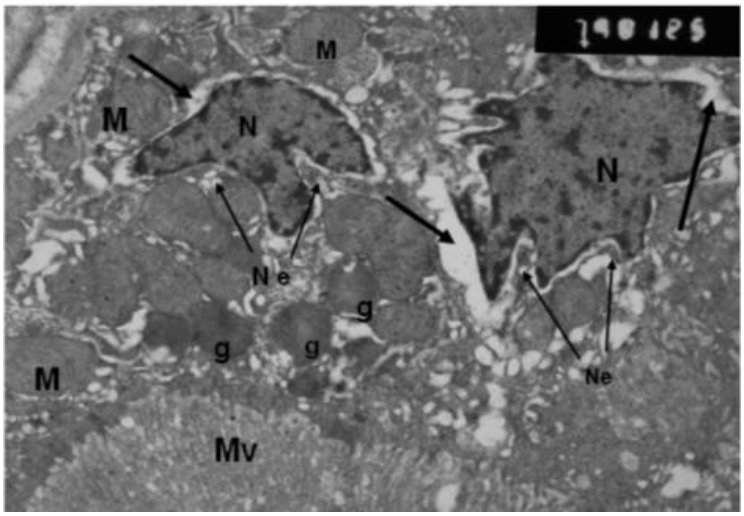

Figure 24. Electron micrograph of a proximal convoluted tubule cell in the kidney of mouse treated with 0.3 mg/kg BW cisplatin, showing two pyknotic nuclei (N) having no nucleoli; Note: different sizes and shapes of mitochondria (M); arrows point at the perinuclear spaces; many dense granules (g) in the cytoplasm; microvilli (Mv), × 7500.

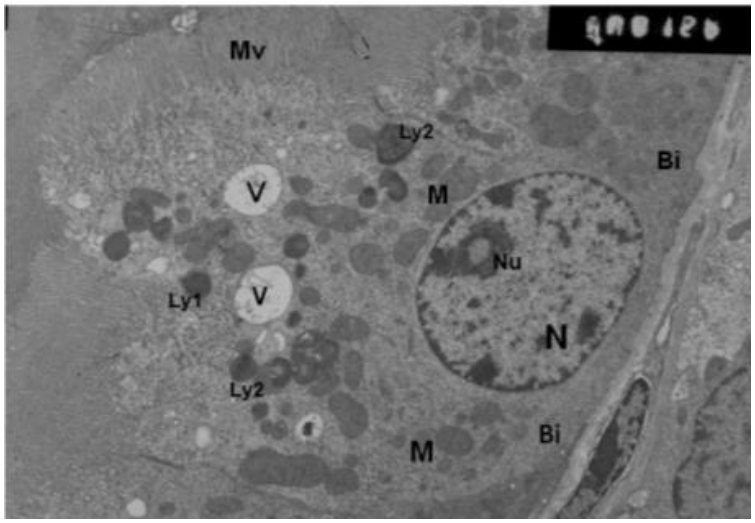

Figure 25. Electron micrograph of a proximal convoluted tubule cell in kidney of mouse treated with 0.3 mg/kg BW cisplatin, showing the disarrangement of the mitochondria (M); Note: the basally-located nucleus (N) contains compact nucleolus (Nu); primary secondary lysosomes (Lys); large vacuoles (V); microvillus (Mv), × 5000.

aberrations in metaphase were significantly increased in mice treated with 0.3 mg/kg BW cisplatin. These chromosomal aberrations were mainly performed in the formation of chromatid breakages (deletion, gap, break and fragment). Febrer et al. (2008) explained that the chromosomal damage after G1 stage of the cell cycle causes chromatid damages and chromatid breakage. Ito and Matsumoto (2010) explained that the centromeric attenuation of chromosomes as an indication for splitting of the centromere without mitosis may be an early stage of endomitosis, in which case it gives rise to polyploidy. This increase in centromerically chromosomal attenuation indicated the effect of cisplatin on the spindle apparatus and the polyploidy (Nersesyan et al., 2003; Misra and Choudhury, 2006).

The current results indicated histological and

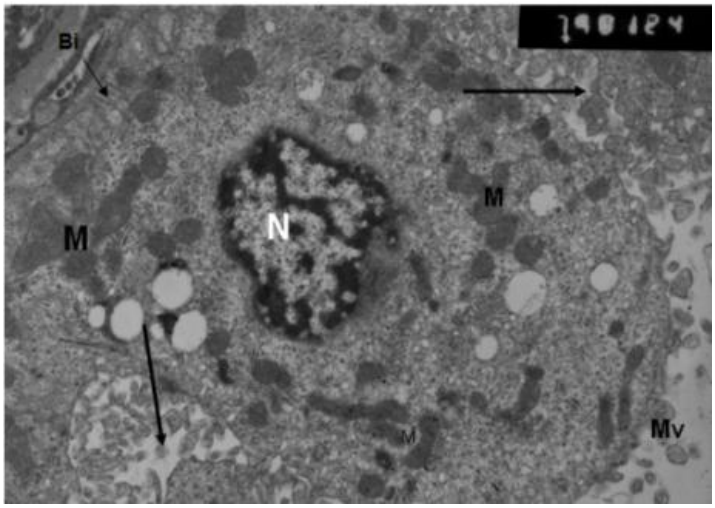

Figure 26. Electron micrograph of a distal convoluted tubule cell in the kidney of mouse treated with 0.3 mg/kg BW containing pyknotic nucleus (N); Note: the cytoplasm contains many lager vacuoles (V) and pleomorphic mitochondria (M), × 3000.

ultrastructural changes of the cortical region of kidney of mice treated with the two different doses of cisplatin. These changes include severe atrophy in the glomeruli; rupture of Bowman's capsule and dilatation in the urinary space. These results are confirmed by the report documented by Ravindra et al. (2010) who demonstrated that cisplatin could induce acute renal necrosis with marked congestion of the glomeruli and glomerular atrophy. Karimi et al. (2005) found that 3 mg/kg cisplatin for 5 days showed severe tubular necrosis among kidney sections of rats. In addition, there was progressive tubular damage in both proximal and the distal convoluted tubules, manifested in fragmented microvilli, increased frequency of pyknotic nuclei, cytoplasmic vacuolization, increased lysosomes and changes in the mitochondrial structure and arrangement. Behling et al. (2006) suggested that cisplatin acts mostly on the proximal convoluted tubules. Shalaby et al. (2006) found degenerative changes in the proximal convoluted tubules in the kidney of male albino mice administered with cisplatin over 21 days. Kim et al. (1995) had reported that cisplatin caused nephrotoxicity which was evidenced by significant loss of brush-border microvilli which is supposed to be responsible for reducing the area for active glucose reabsorption (Devipriya and Shamala, 1999). The mesangium cells were characterized by highly electron dense mesangial matrix. These data are in close correlation with those reported by Kohn et al. (2002) who studied the nephrotoxic effect of cisplatin on kidney glomerular components in guinea pigs. Moreover, the present results revealed that the mesangial cells appeared irregular with bizarre shaped nuclei and dense matrices. It is conceivable that even a minor reduction in the mesangial cell area could affect the filtering surface of the glomeruli and explained the decrease in the glomerular filtration (Rodriguez-Barbero et al., 2000).

Further, the current results revealed marked focal loss in the brush border, pyknotic nuclei, chromatin condensation, swelling of the mitochondria with regression of the mitochondrial cristea, in addition to the increased number of lysosomes. However, there were much less distal convoluted tubules changes, including minimal microvilli, pyknotic nuclei and organelles disorganization. Abdelmeguid et al. (2010) revealed great similarities to a certain extent with the results of this study, where cisplatin resulted in focal and severe tubular changes in PCT and DCT cells, in male albino mice.

In conclusion, the results of the current study suggest that cisplatin could induce nephrotoxicity, causing DNA damage, appearance of chromosomal aberrations, and ultrastructural alterations in all parts of the renal tubules and the renal corpuscles. This indicates that other new chemothertapeutic drugs should be discovered in order to decrease their possible toxic side effects on the human health.

REFERENCES

Abdelmeguid NE, Chmaisse HN, Abou ZNS (2010). Protective effect of silymarin on cisplatin-induced nephrotoxicity in rats. Pak. J. Nutr., 9(7): 624-636.

Abdelwahab HMF, Hassanin NIY, Ahmed EM, Abd-El-Monem AR (2011). Impact of consuming each of dried black grape and hot red pepper alone or in combination on nephrotoxicity induced by cisplatin injection in rats. Aust. J. Basic Appl. Sci., 5(10): 231-238.

Ajith TA, Usha S, Nivitha V (2007). Ascorbic acid and a-tocopherol protect anticancer drug cisplatin

induced nephrotoxicity in mice. a comparative study. Clin. Chim. Acta., 375: 82-86.
Ali BH, Al-Moundhri MS (2006). Agents ameliorating or augmenting the nephrotoxicity of cisplatin and other platinum compounds: a review of some recent research. Food Chem. Toxicol., 44: 1173-1183.
Atessahin A, Yilmaz S, Karahan I, Ceribasi AO, Karaoglu A (2005). Effects of lycopene against cisplatin-induced nephrotoxicity and oxidative stress in rats. Toxicology, 212: 116-123.
Bancroft JD, Gamble M (2002). Theory and Practice of Histological Techniques. 5th (Ed.) Churchill Livingstone, London, p. 153.
Behling EB, Milena CS, Heloísa DCF, Lusânia MGA, Roberto SC, Maria de Lourdes PB (2006). Comparative study of multiple dosage of quercetin against cisplatin-induced nephrotoxicity and oxidative stress in rat kidneys. Pharmacol. Rep., 58: 526-532.
Chandrasekar MJN, Bommu P, Nanjan MJ, Suresh B (2006). Chemoprotective effect of *phyllanthus maderaspatensis* in modulating cisplatin-induced nephrotoxicity and genotoxicity. J. Phar. Bio., 44(2): 100-106.
Custódio JB, Cardoso CM, Santos MS, Almeida LM, Vicente JA, Fernandes MA (2009). Cisplatin impairs rat liver mitochondrial functions by inducingchanges on membrane ion permeability: prevention by thiol group protectingagents. Toxicology, 259: 18-24.
Devipriya S, Shamala D (1999). Protective effects of quercetin in cisplatin-induced cell injury in the rat kidney, Ind. J. Pharmacol., 3: 422-426.
Domitrovic R, Potocˇnjak I, Crncˇevic´-Orlic Z, Škoda M (2014). Nephroprotective activities of rosmarinic acid against cisplatin-induced kidney injury in mice. Food Chem. Toxicol., 66: 321-328.
Dzagnidze A, Katsarava Z, Makhalova J, Liedert B, Yoon M, Kaube H, Limmroth V, Thomale J, (2007). Repair Capacity for Platinum-DNA Adducts Determines the Severity of Cisplatin-Induced Peripheral Neuropathy. J. Neurosci., 27(35): 9451-9457.
Febrer E, Mestres M, Caballín MR, Barrios L, Ribas M, Gutiérrez-Enríquez S, Alonso C, Ramón Y, Cajal T, Francesc BJ (2008). Mitotic delay in lymphocytes from BRCA1 heterozygotes unable to reduce the radiation-induced chromosomal damage. DNA Repair (Amst), 7: 1907-1911.
Florea AM, Büsselberg D (2011). Cisplatin as an Anti-Tumor Drug: Cellular Mechanisms of Activity, Drug Resistance and Induced Side Effects. Cancers, 3: 1351-1371.
Hassan I, Chibber S, Naseem I (2010). Ameliorative effect of riboflavin on the cisplatin induced nephrotoxicity and hepatotoxicity under photoillumination. Food Chem. Toxicol., 48: 2052-2058.
Hayat MA (2000). Principles and techniques of electron microscopy: Biological applications. 4th ed. Cambridge: Cambridge University Press, pp 24-96.
Holland JF, Bast RC, Morton DL, Frei E, kufe DW, Weichselbaum RR (1997). Chemotherapeutic agents. In Cancer Medicine. 4th ed. (Williams & Wilkins, Baltimore, MD), pp. 907-1045.
Ito D, Matsumoto T (2010). Molecular mechanisms and function of the spindle checkpoint, a guardian of the chromosome stability. Adv. Exp. Med. Biol., 676: 15-26.
Karimi G, Ramezani M, Tahoonian Z (2005). Cisplatin nephrotoxicity and protection by milk thistle extract in rats. Evidence Based Complement Alternat. Med., 2: 383-386.
Kim YK, Byun HS, Kim YH, Woo JS, Lee SH (1995). Effect of cisplatin on renal function of rabbits: mechanism of reduced glucose reabsorption, Toxicol. Appl. Pharmacol., 130: 19-26.
Kohn S, Fradis M, Ben-David J, Zidan J, Robinson E (2002). Nephrotoxicity of combined treatment with cisplatin and gentamicin in the guinea pig: Glomerular injury findings. Ultrastructural Pathol., 26: 371-382.
Mansour HH, Hafez FH, Fahmy NM (2006). Silymarin modulates cisplatin-induced oxidative stress and hepatotoxicity in rats. J. Biochem. Mol. Biol., 39: 656-661.
Miller RP, Tadagavadi RK, Ramesh (2010). Mechanisms of cisplatin nephrotoxicity. Toxins (Basel), 2: 2490-2518.
Misra S, Choudhury RC (2006). Vitamin C modulation of cisplatin-induced cytogenotoxicity in bone marrow, spermatogonia and its transmission in the male germline of Swiss mice. J. Chemother., 18: 182-187.
Nersesyan A, Perrone E, Roggieri P, Bolognesi C, (2003). Genotoxic action of cycloplatam, a new platinum antitumor drug, on mammalian cells *in vivo* and *in vitro*. Chemother., 49: 132-137.
Park MS, Maryely DL, Devarajan P (2002). Cisplatin induces apoptosis in LLC-PK1 cells via activation of mitochondrial pathways. J. Am. Soc. Nephrol., 13: 858-865.
Preston RJ, Dean BJ, Galloway S, Holden H, McFree AF, Shelby M (1987). Mammalian in vivo cytogenetic assays: analysis of chromosome aberrations in bone marrow cells. Mutat. Res., 189: 157-165.
Ravindra P, Bhiwgade DA, Kulkarni S, Rataboli V, Dhumem Y (2010). Cisplatin induced histological changes in renal tissue of rat. J. Cell Anim. Biol., 4(7): 108-111.
Rodriguez-Barbero A, L'Azou B, Cambar J, Lopez-Novoa JM (2000). Potential use of isolated glomeruli and cultured mesangial cells as in vitro models to assess nephrotoxicity. Cell Biol. Toxicol., 16: 145-153.
Saad AA, Youssef MI, El-Shennawy LK (2009). Cisplatin induced damage in kidney genomic DNA and nephrotoxicity in male rats: The protective effect of grape seed proanthocyanidin extract. J. Food Chem. Toxicol., 47: 1499-1506.
Sahu BD, Reddy KKR, Putcha UK (2011). Carnosic acid attenuates renal injury in an experimental model of rat

cisplatin-induced nephrotoxicity. Food Chem. Toxicol., 49: 3090–3097.
Shah N, Dizon DS (2009). New-generation platinum agents for solid tumors. Future Oncol., 5: 33-42.
Shalaby T, Ghanem AM, Ramadan HS (2006). Cytotoxicity changes of cisplatin drug in the presence of magnetic fields. Romanian J. Biophys., 4: 229-241.
Tikoo K, Bhatt DK, Gaikawad AB, Sharma V, Kabra DG (2007). Differential effects of tannic acid on cisplatin induced nephrotoxicity in rats. FEBS Letters, 581: 2027–2035.
Yoshida J, Kosaka H, Tomioka K, Kumagai S (2006). Genotoxic risks to nurses from contamination of the work environment with antineoplastic drugs in Japan. J. Occup. Health, 48: 517-522.
Zhang J, Wang L, Xing Z, Liu D, Sun J, Li X, Zhang Y (2010). Status of bi- and multi-nuclear platinum anticancer drug development. Anticancer Agents Med. Chem., 10: 272–282.